한국공작기계학회 '99년도 춘계학술대회 논문집 pp.63~68

공작기계 상에서의 측정시스템의 설계

Synthesis of the Measurement System on the Machine Tool

정성종*(한양대 기계공학부), 김경돈(한양대 대학원 기계설계학과)

Sung-Chong Chung*, Kyung-Don Kim

ABSTRACT

A 2½ dimensional measurement and inspection system realized on the machine tool using a touch trigger probe and measuring G codes is synthesized in this paper. Measuring G codes have been constructed according to geometric forms, precision attributes, relationships between two parts, datum hierarchies, and relevant technological data by using measuring arguments. Algorithms for calibration and compensation of measuring errors are proposed to ensure the measuring accuracy by using a laser interferometer and ring gauges. Classification of feedrates according to the objectives of movement makes it possible to reduce measuring time and also implement collision-free measurement. Experiments are conducted to verify the validity and effectiveness of proposed methods

1. INTRODUCTION

On-machine inspection systems can be used to inspect dimensional errors of workpieces with respect to design requirements on the machine tools. Efforts have been devoted to develope accurate and rapid measurement systems on the machine tools[1~4]. Many kinematic reference standards and artefacts such as magnetic ball bars, master disks and ball plates have been used to calibrate the accuracy of machine tools[2~6]. In order to reduce measuring time of inspection processes, some of research works have been studied on coordinate measuring machines [7~8].

In this paper, we propose a design methodology of the 2½ dimensional measurement and inspection system realized on the machine tool using a touch trigger probe and measuring G codes. Items considered in the system design are 1) accuracy insurance of measuring results, 2) reduction of measuring time and countermeasure for probe protection, and 3) improvement of measuring and inspection processes.

Algorithms for calibration and compensation of measuring errors are proposed to enhance measuring accuracy by using a laser interferometer and ring gauges. Classification of feedrates according to the objectives of movement can reduce measuring time and implement collision-free measurements. All functions needed for measurement and inspection processes have been constructed as measuring G codes, which have similar forms with machining G codes. Arguments of measuring G codes are as follows: geometric forms, precision attributes, relationships between two parts, datum hierarchies, and relevant technological data. Comparing the developed system with the previous on-machine measurement and inspection system[9], problems such as difficulties in management of measuring part programs, needs of experts and the frequent walk between a CNC and a PC can be minimized through the measuring G codes. The validity and effectiveness of the developed system has been confirmed on a vertical machining center.

2. MEASURING ERRORS

Fig. 1 shows measuring errors generated due to discrepancy between the ideal contact point and the position recognized by a CNC on the machine tool. These measuring errors are caused by geometric errors of the machine tool, probing errors, and fixing errors of a probe assembly. The probing errors mean probe lobing errors and axis reversal errors[3].

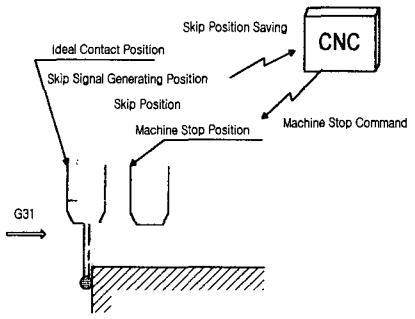

Fig. 1 Measuring mechanism.

Fig. 2 shows a typical error pattern due to measuring errors when a ring gage is probed with a touch trigger probe on the machine tool. The fixing error of a probe assembly will not be

considered in this paper, because it can be removed easily by coinciding the center of a spindle axis to that of a stylus tip. Calibration and compensation of the probing errors and the geometric errors will be discussed in the following.

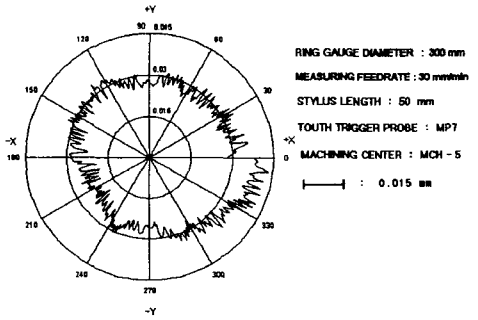

Fig. 2 Typical measuring error pattern.

When a probe is commanded to move itself from the origin $O'(X_0, Y_0, Z_0)$ in measuring work coordinates to the ideal contact point $I(X, Y, Z)$, which is away from the origin by R, the actual contact point $S(X', Y', Z')$ measured by a skip signal is depicted as shown in Fig. 3(a). The error vector $\vec{E}$ represents a summation of the geometric and the probing error. That is,

$$\vec{E} = [E_X\ E_Y\ E_Z]^T = \vec{E}_G + \vec{E}_P = \vec{P}_{skip} - \vec{P}_{ideal} \quad (1)$$

where, $E_X = E_{GX} + E_{PX} = X' - X$
$E_Y = E_{GY} + E_{PY} = Y' - Y$
$E_Z = E_{GZ} + E_{PZ} = Z' - Z$

In eq.(1), the geometric error, $\vec{E}_G = \vec{E}_G(X, Y, Z)$, is a function of axis position of a machine tool, and the probing error, $\vec{E}_P = \vec{E}_P(F_m, \theta)$, is a function of probing feedrate and direction.

When this concept of volumetric errors is applied to the ring gauge on the machine tool as shown in Fig. 3(b), the following relationship is established,

$$R^2 = (X - X_0)^2 + (Y - Y_0)^2 \quad (2)$$

However, $\vec{P}_{skip}$ means the actual measured position. So that the actual distance between the origin O' and the ideal contact point $I(X, Y, Z)$ has to be $R + \triangle R$. That is,

$$(R + \triangle R)^2 = (X' - X_0)^2 + (Y' - Y_0)^2 = (X - X_0 + E_X)^2 + (Y - Y_0 + E_Y)^2 \quad (3)$$

where $\triangle R$ represents the radius error due to the measurement of a ring gauge.

Substituting eq. (1) and (2) into eq. (3) and neglecting higher order terms, the radius error of eq. (3) can be rewritten in terms of the geometric and the probing errors as follows:

$$\triangle R = \frac{1}{R}\{(X - X_0)(E_{GX} + E_{PX}) + (Y - Y_0)(E_{GY} + E_{PY})\} = \left\{\frac{(X - X_0)}{R} E_{GX} + \frac{(Y - Y_0)}{R} E_{GY}\right\} + \left\{\frac{(X - X_0)}{R} E_{PX} + \frac{(Y - Y_0)}{R} E_{PY}\right\} \quad (4)$$

If the size of a ring gauge on the machine tool is relatively small, geometric errors can be assumed to be very small, and then it can be neglected in the measurement of a small ring gauge. In this case, radius error $\triangle R$ of eq. (4) can be rewritten in terms of probing errors as follows:

$$\triangle R_P = \left\{\frac{(X - X_0)}{R} E_{PX} + \frac{(Y - Y_0)}{R} E_{PY}\right\} = E_{PX}\cos\theta + E_{PY}\sin\theta \quad (5)$$

By measuring a ring gauge with 30mm diameter, repeatable probing errors E_{PX} and E_{PY} can be identified from measured radius errors according to measuring direction θ.

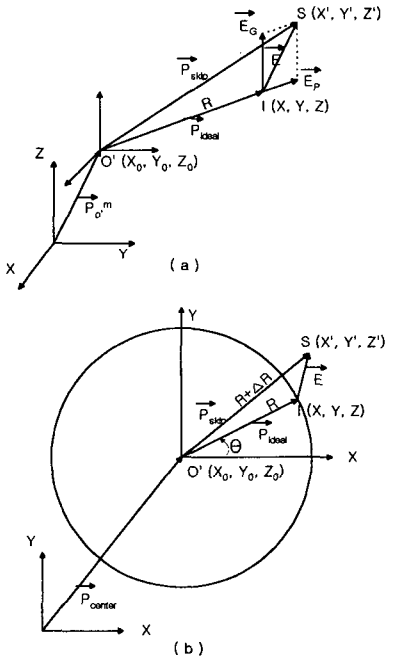

Fig. 3 (a) Volumetric measuring errors. (b) Calibration of measuring errors using a ring gauge.

Two ways are applied to calibrate and compensate for geometric errors.

The first is the calibration of pitch errors of ball screws by using a laser interferometer, and then compensated for with modifying pitch error parameters of a CNC. Fig. 4 shows compensation results of pitch errors. However, this procedure is required for accurate assessment of squareness errors and scale errors, frequent operations of the

pitch error compensation is not needed because basic profiles of pitch errors are repeatable and not changed drastically.

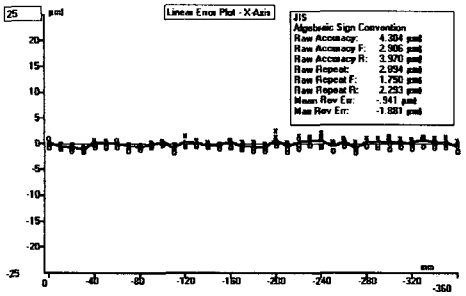

(a) X-Axis.

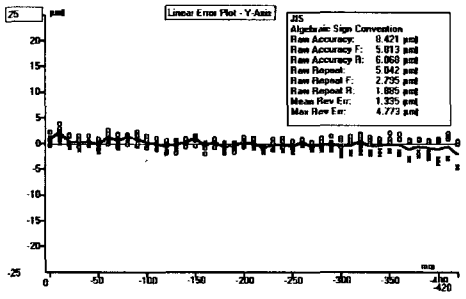

(b) Y-Axis.

Fig. 4 Pitch error compensation using a laser interferometer.

The second is the calibration of a squareness error between two perpendicular axes and linear thermal expansion errors of positioning scales. A ring gauge with large size is used to include sufficient amount of geometric errors within the working volume. After compensating for probing errors of eq. (5), radius errors due to geometric errors of eq. (4) is given by

$$\triangle R_G = \left\{ \frac{(X-X_0)}{R} E_{GX} + \frac{(Y-Y_0)}{R} E_{GY} \right\} \quad (6)$$

Considering a squareness error and linear thermal expansions of positioning scales within intervals of $X_0 - R \le X \le X_0 + R$ and $Y_0 - R \le Y \le Y_0 + R$,

$$E_{GX} = \frac{e_x}{R}(X-X_0) + (Y-Y_0)\tan\alpha \quad (7)$$
$$E_{GY} = \frac{e_y}{R}(Y-Y_0)$$

where, e_x, e_y : linear thermal expansion of positioning scale
α : squareness error

Substituting eq. (7) into eq. (6), radius errors due to geometric errors can be obtained as follows:

$$\triangle R_G = \frac{e_x}{R^2}(X-X_0)^2 + \frac{\tan\alpha}{R}(X-X_0)(Y-Y_0) + \frac{e_y}{R^2}(Y-Y_0)^2 \quad (8)$$

After a ring gauge with 300mm diameter is probed and the radius error of eq. (4) are calibrated through the probing error of eq. (5), e_x, e_y and α can be computed by comparing the calibrated radius error with the radius error of eq. (8). Finally, geometric errors of a machine tool can be identified from eq. (7).

By using eq. (1) and the calibrated error vector $\vec{E}$, probed values can be compensated effectively for according to the measuring position and direction.

3. MEASURING TIME

In order to minimize measuring time under high quality measurement environment, probing feedrates have to be classified according to probe paths. Three kinds of feedrates are designed as follows: rapid feedrate, jog feedrate and measuring feedrate. The rapid feedrate is to let the probe move with available maximum speed between two different measuring locations. In order to compensate for alignment errors of a workpiece on the machine tool, the jog feedrate is to move the probe to get to an approximate touching point of the workpiece with high speed. The measuring feedrate is used to take an accurate measurement of the workpiece dimension based on the approximate touching point acquired during the jog feedrate process. In this paper, the measuring feedrate is adopted as the feedrate, which is recommended as the best feedrate during touching process[9].

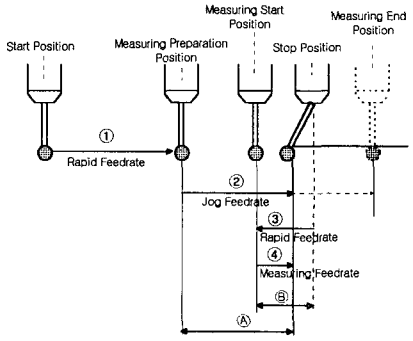

Fig. 5 Classification of feedrates.

As shown in Fig. 5, a measuring preparation point, which is a boundary between the rapid feedrate and the jog feedrate, is away from the workpiece by Ⓐ. A measuring start point is away from the stop position by Ⓑ. Ⓐ means a summation of the acceleration range required for

the jog feedrate, the tolerance range of the workpiece alignment error and the radius of stylus tip. Ⓑ represents a summation of the distance between a touching point and a probe stop position at the jog feedrate, the acceleration range required for the measuring feedrate and the radius of a stylus tip.

Required acceleration ranges can be determined with experiments. A ring gauge is used so that the distance between a current probe position and an ideal touching point can be easily acquired. The abscissa of Fig. 6 represents the probe start position which is the distance between a current probe position and an ideal touching point, and the ordinate represents skip positions. When skip positions reach steady states, the probe start positions become the acceleration ranges.

The probe stops within 16msec in the Fanuc CNC, right after the CNC detects a skip signal. The distance between the workpiece and the probe stop point can be determined as follows[10]:

$$Q_{max} = S_p + F_m \times 1/60 \times 16/1000 \quad (9)$$

where, Q_{max} : maximum stop position (mm)
S_p : skip position (mm)
F_m : feedrate (mm/min)

If a probe collides with a workpiece unexpectedly, a probe assembly can be damaged or fractured. In order to protect the probe from accidents, a probe-collision-check algorithm is required as follows. When a probe moves at the rapid feedrate, basically, it is pulled out to a conservatively selected safety clearance zone and skip signal is monitored during the whole path. However, a stylus will be fractured if the stylus is collided with the workpiece by a mistake and the probe exceeds the predetermined overtravel limit. Hence, the rapid feedrate should be chosen as a feedrate, which is the fastest feedrate in the range where Q_{max} of eq. (9) is smaller than the predetermined overtravel limit. Finally, if a skip signal is detected at any position, and current skip position is much different from the commanded workpiece position, the developed system recognizes that the probe collides with the workpiece, and then displays error message.

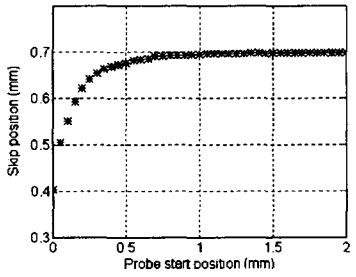

Fig. 6 Determination of acceleration range.

In this study, rapid feedrate is chosen as 4 m/min, jog feedrate as 2 m/min, and measuring feedrate as 30 mm/min. And the probe is moved along the path of ①→②→③→④ as shown in Fig. 5. Hence, reduction of measuring time, with measurement quality being maintained high, can be achieved with manipulation of feedrates.

4. MEASURING G CODES

Measuring G codes from G100 to G104 have been designed for measuring preparation functions (group 1), which include compensation of measuring errors, selection of work coordinates, and so on. Codes from G105 to G108 are assigned to basic measuring features (group 2), which include circle, pocket, web, corner, and plane. G109 is allotted to applied measurements (group 3), which analyzes relationships between two basic measuring features in group 2.

Fig. 7 shows a classification of measuring G codes. The argument A divides G codes into different measuring features. The probing feature and posture is classified according to the argument Q.

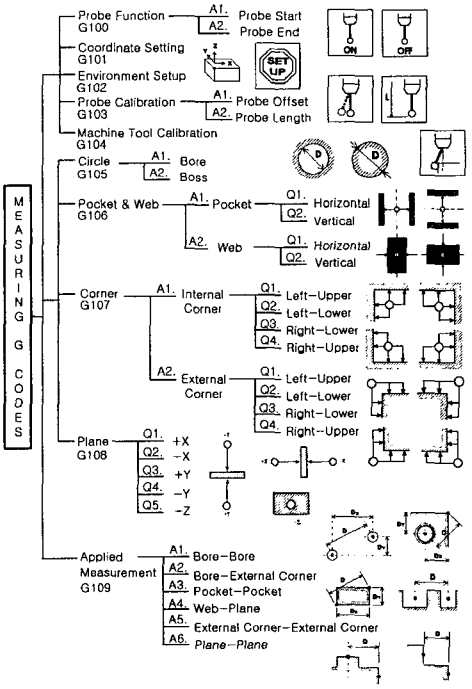

Fig. 7 Classification of measuring G code.

The precision attributes are specified with the following manner to determine the position and the size of measuring features.

```
// Precision attributes
Precision ( FEATURE . POSITION ) {
  UPPER_LIMIT_TOLERANCE ( R {mm} );
```

```
  LOWER_LIMIT_TOLERANCE ( S {mm} );
  REFERENCE_POSITION ( X, Y, Z );
}
Precision ( FEATURE . SIZE ) {
  UPPER_LIMIT_TOLERANCE ( U {mm} );
  LOWER_LIMIT_TOLERANCE ( V {mm} );
  REFERENCE_SIZE ( D or H {mm} );
}
```

The reference position in the above precision attributes is selected to be relative to the work coordinates defined as follows:

```
// Datum hierarchies
Datum ( FEATURE . COORDINATES ) {
  WORK_COORDINATES ( W );
}
```

All measuring informations of each measuring feature are saved in the memory according to the item number of each measuring feature. Thus, relationships between two basic measuring features are deduced from relationships between two parts which include item numbers as follows:

```
// relationships between two parts
Relation ( FEATURE1_FEATURE2 . DISTANCE ) {
  FEATURE1_ITEM_NUMBER ( C );
  FEATURE2_ITEM_NUMBER ( K );
  DISTANCE_BETWEEN_FEATURES ( D {mm} );
  X_AXIS_DISTANCE ( X {mm} );
  Y_AXIS_DISTANCE ( Y {mm} );
}
```

Technological data such as the item number, informations of the probe, axis moving length and measuring procedure are given by

```
// Relevant technological data
Technology ( FEATURE . ITEM ) {
  ITEM_NUMBER ( E );
}
Technology ( FEATURE . PROBE ) {
  PROBE_NUMBER ( T );
  STYLUS_DIAMETER ( D {mm} );
  STYLUS_LENGTH ( H {mm} );
}
Technology ( FEATURE . MOVE ) {
  X_AXIS_MOVE_LENGTH ( I {mm} );
  Y_AXIS_MOVE_LENGTH ( J {mm} );
}
Technology ( FEATURE . PROCEDURE ) {
  MEASURING_PROCEDURE ( B );
}
```

All attributes are represented as arguments of measuring G codes according to required informations of measuring features. Table 1 shows measuring G codes and arguments according to measuring features. Measuring G codes are potted in a ROM of the Fanuc CNC, and they are called to perform an operation by the CNC without interfacing with PCs.

Table 1 Measuring G codes.

Measuring Features	Measuring G codes
1. Probe Start 2. Probe End 3. Coordinate Setting 4. Environment Setup 5. Probe Offset 6. Probe Length 7. Machine Tool Calibration	G100 A1. D□ H□ T□ G100 A2. G101 D□ W□ G102 E□ I□ J□ K□ T□ G103 A1. B□ D□ E□ T□ G103 A2. B□ E□ H□ T□ G104 D□ E□ T□ W□ X□ Y□ Z□
8. Bore 9. Boss 10. Pocket 11. Web 12. Internal Corner 13. External Corner 14. Plane (X, Y, Z)	G105 A1. D□ E□ R□ S□ U□ V□ W□ X□ Y□ Z□ G105 A2. D□ E□ R□ S□ U□ V□ W□ X□ Y□ Z□ G106 A1. E□ H□ Q□ R□ S□ U□ V□ W□ X□ Y□ Z□ G106 A2. E□ H□ Q□ R□ S□ U□ V□ W□ X□ Y□ Z□ G107 A1. E□ I□ J□ Q□ R□ S□ W□ X□ Y□ Z□ G107 A2. E□ I□ J□ Q□ R□ S□ W□ X□ Y□ Z□ G108 E□ Q□ R□ S□ W□ X□ Y□ Z□
15. Bore-Bore 16. Bore-Ex.Cor. 17. Pocket-Pocket 18. Web-Plane 19. Ex.Cor.-Ex.Cor. 20. Plane-Plane	G109 A1. C□ D□ E□ K□ U□ V□ X□ Y□ G109 A2. C□ D□ E□ K□ U□ V□ X□ Y□ G109 A3. C□ D□ E□ K□ U□ V□ G109 A4. C□ D□ E□ K□ U□ V□ G109 A5. C□ D□ E□ K□ U□ V□ X□ Y□ G109 A6. C□ D□ E□ K□ U□ V□

5. EXPERIMENT

To verify the validity and effectiveness of the proposed methods, experiments are performed by comparing the developed system with the coordinate measuring machine. Table 2 shows measuring conditions and specifications of the experimental setup.

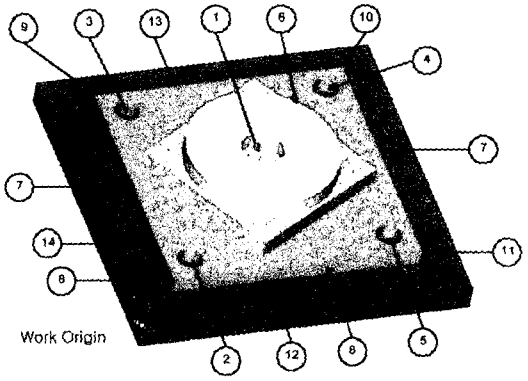

Fig. 8 Artefact for comparison test

An artefact has been designed for experiments. Fig. 8 shows the artefact and its measuring features for comparison tests. The overall dimensions are of $400 \times 400 \times 90$mm.

Table 2 Specification of experimental setup.

	Developed System	CMM
Measuring Machine	Horizontal Machining Center with Fanuc 15MA (Tongil Heavy Industry : MCH-5)	Coordinate Measuring Machine (Carl Zeiss : UMM550)
Probe	MP7 Touch Trigger Probe Stylus Length : 50mm Stylus Tip Diameter : 6mm	Stylus Length : 50mm Stylus Tip Diameter : 6mm
Method	Interactive Measuring Part Progamming	Automatic Programming
Environment	Actual Working Environment	Constant Temperature and Humidity

Table 3 Comparison of developed system with CMM

Measuring Feature	Item Number	Measuring Results (mm)				Measuring Time	
		Size (Developed System)	Center Position (Developed System)	Size Error (CMM-Developed System)	Center Position Error (CMM-Developed System)	Developed System	CMM
Bore	①	ϕ 50.012	(200.001, 200.003)	0.0032	(0.0018, 0.0014)	3'52"	3'57"
	②	ϕ 30.007	(80.001, 80.000)	0.0025	(-0.0004, -0.0007)	3'28"	3'30"
	③	ϕ 30.008	(80.001, 320.004)	-0.0017	(0.0021, -0.0013)	3'34"	3'40"
	④	ϕ 30.007	(320.003, 320.006)	0.0021	(0.0026, 0.0034)	3'35"	3'42"
	⑤	ϕ 30.007	(320.005, 80.002)	0.0006	(0.0014, -0.0008)	3'33"	3'40"
Boss	⑥	ϕ 179.989	(200.002, 200.003)	-0.0039	(-0.0035, -0.0012)	4'27"	5'02"
Horizontal Web	⑦	300.002	X : 200.001	0.0034	0.0015	3'12"	3'27"
External Corner	⑧	-	(50.000, 50.001)	-	(-0.0003, -0.0007)	3'21"	4'16"
	⑨	-	(50.001, 350.005)	-	(0.0014, -0.0031)	3'32"	4'24"
	⑩	-	(350.004, 350.006)	-	(0.0025, 0.0021)	3'34"	4'30"
	⑪	-	(350.006, 50.002)	-	(0.0020, -0.0011)	3'30"	4'25"
Plane	⑫	-	Y : 50.002	-	0.0017	3'07"	3'05"
	⑬	-	Y : 350.006	-	-0.0023	3'12"	3'08"
Bore-Bore	②③	240.004	-	-0.0006	-	0'28"	0'35"
	②⑤	240.004	-	0.0018	-	0'27"	0'30"
	②④	339.417	-	0.0049	-	0'27"	0'29"
Bore-External Corner	①⑧	212.134	-	0.0031	-	0'28"	0'46"
	②⑧	42.426	-	0.0003	-	0'25"	0'41"
External Corner-External	⑧⑨	300.004	-	-0.0024	-	0'26"	0'52"
	⑧⑪	300.006	-	0.0023	-	0'27"	0'45"
Corner Plane - Plane	⑧⑩	424.270	-	0.0044	-	0'26"	0'47"
	⑫⑬	300.004	-	-0.0040	-	0'28"	0'35"

Table 3 shows comparisons of measuring results and measuring times between the developed system and the coordinate measuring machine. Since the geometric and the probing errors of the developed system are calibrated and compensated for, measuring accuracy of the developed system becomes within $\pm 5\mu m$ against that of the coordinate measuring machine. This is due to repeatable and random errors of the positioning devices and the probes. By using the classified feedrates for probing and the measuring G codes, we can also reduce measuring time as shown in Table 3.

6. CONCLUSIONS

After designing and analyzing 2½ dimensional measurement and inspection system on the machine tool, following conclusions are obtained:

(1) Algorithms for calibration and compensation of measuring errors by a laser interferometer and ring gauges have been proposed for enhancing measuring accuracy. By making use of proposed methods, calibrations are performed well and rapidly.

(2) Classification of feedrates into the rapid feedrate, the jog feedrate and the measuring feedrate reduces measuring time and implement collision-free measurements.

(3) All functions required for measurement and inspection processes have been designed as measuring G codes with similar forms of machining G codes. Measuring G codes are potted in a ROM of the CNC. Measuring commands are generated on the screen of the CNC without PC interface.

(4) The validity and effectiveness of the developed algorithms has been demonstrated by comparing performances of the developed system with that of the coordinate measuring machine.

REFERENCES

(1) Y. Kakino and Y. Ihara, 1990, "Development of Machining and Measuring Center and Evaluation of its Performance", *Proceedings of Japan-USA Symposium on Flexible Automation*, pp 189~195.

(2) S. C. Chung and K. D. Kim, 1998, "Design and Implementation of an On-the-Machine Measuring and Inspection Module", *KSPE*, Vol. 15, No. 4, pp.91~97. (in Korean)

(3) K. D. Kim and S. C. Chung, 1999, "Design and Analysis of 2½ Dimensional On-the-Machine Measuring and Inspection System using Touch Trigger Probes", *Transactions of the KSME A*, Vol. 23, No. 1, pp. 37~46. (in Korean)

(4) J. Mou and C. R. Liu, 1992, "A Method for Enhancing the Accuracy of CNC Machine Tools for On-Machine Inspection", *Journal of Manufacturing Systems*, Vol. 11, No. 4, pp. 229~237.

(5) J. Bryan, 1982, "A Simple Method for Testing Measuring Machines and Machine Tools", *Precision Engineering*, Vol. 4, No. 2, pp.61~69.

(6) W. Knapp, 1983, "Circular Test for Three Coordinate Measuring Machines and Machine Tools", *Precision Engineering*, Vol. 5, pp.115~124.

(7) E. Lu, J. Ni and S. M. Wu, 1994, "An Algorithm for the Generation of an Optimum CMM Inspection Path", *Journal of Dynamic Systems, Measurement, and Control*, Vol. 116, pp.396~404.

(8) S. D. Jones and A. G. Ulsoy, 1995, "An Optimization Strategy for Maximizing Coordinate Measuring Machine Productivity", *Journal of Engineering for Industry*, Vol. 117, pp.601~618.

(9) Renishaw, 1988, *Renishaw Programming Manual*, Gloucestershire, England.

(10) FANUC, 1990, *Series 15 Operating Manual*, ChangWon, Korea.